Renewable Energy 96 (2016) 377–389

Contents lists available at ScienceDirect

Renewable Energy

journal homepage: www.elsevier.com/locate/renene

A comparative study of evolutionary algorithms and adapting control parameters for estimating the parameters of a single-diode photovoltaic module's model

Dhiaa Halboot Muhsen [a, b, *], Abu Bakar Ghazali [a], Tamer Khatib [c], Issa Ahmed Abed [d]

[a] Department of EC Engineering, University of Tenaga Nasional, Malaysia
[b] Department of Computer and Software Engineering, University of Al- Mustansiriyah, Iraq
[c] Department of Energy Engineering and Environment, An-Najah National University, Palestine
[d] Engineering Technical College Basrah, Southern Technical University, Iraq

ARTICLE INFO

Article history:
Received 15 October 2015
Received in revised form
5 February 2016
Accepted 24 April 2016
Available online 7 May 2016

Keywords:
Differential evolution
Electromagnetism-like
Parameter extraction
Photovoltaic
Single-diode model

ABSTRACT

This paper proposes different evolutionary algorithms, such as differential evolution and electromagnetism-like algorithms, to extract the five parameters of a single-diode photovoltaic module's model. Hybrid evolutionary algorithms are proposed with integrated and adaptive mutation per iteration schemes. In addition, a new formula to adjust the mutation scaling factor and crossover rate for each generation is proposed. Analyses are performed based on experimental data points under different weather conditions to explain the robustness and reliability of the proposed methods. Results show that the proposed hybrid algorithms, namely, evolutionary algorithm with integrated mutation per iteration and evolutionary algorithm with adaptive mutation per iteration, exhibit better performance than electromagnetism-like algorithm and other methods in terms of accuracy, CPU execution time, and convergence. The proposed hybrid algorithms offer a root mean square error, mean bias error, coefficient of determination and CPU execution time around 0.062, 0.006 and 0.992, and less than 20 s respectively. Furthermore, the feasibility of the proposed methods is validated by comparing the obtained results with those of other methods under various statistical errors. As a conclusion, the proposed hybrid algorithms offer root mean square error and mean bias error less than other methods by 14% at least.

1. Introduction

Energy crisis, fuel depletion, environmental pollution, and global warming are critical issues in the world that highlight the importance of using alternative energy sources [1]. Solar energy is an environment-friendly, secure, and renewable energy source [2]. Meanwhile, photovoltaic (PV) technology directly utilizes solar radiation and converts it into direct current. Accurate modeling of PV modules is important to design, control, and assess PV systems. The core of a PV module modeling process is estimating equivalent circuit DC parameters. In general, these parameters can be estimated using two types of approach, namely, analytical approaches [3] and numerical approaches [4]. An analytical approach offers simple and fast parameter calculations [5]; however, it is not as accurate as a numerical approach because the simplifications in the numerical approach model do not reflect real operational conditions [6].

Many examples of numerical approaches have been proposed in literature to estimate the parameters of a PV module model. These approaches include the Newton–Raphson method (NR) [7], Levenberg–Marquardt (LM) algorithm [8], artificial neural network (ANN), and fuzzy logic (FL) [9,10]. Hejri et al. [11] proposed a method that combined analytical and NR solutions to extract five parameters of a double-diode PV model based on the specification of the manufacturer of the PV module. However, evolutionary algorithms (EAs) have been recently adopted to estimate the parameters of PV module models after these algorithms have been proven to be the most accurate. Numerous examples of EAs used to estimate the parameters of PV module models are found in literature, including genetic algorithm (GA) [12] and particle swarm

* Corresponding author. Department of EC Engineering, University of Tenaga Nasional, Malaysia.
E-mail addresses: deia_mohussen@yahoo.com (D.H. Muhsen), abakar@uniten.edu.my (A.B. Ghazali), t.khatib@najah.edu (T. Khatib), issaahmedabd80@yahoo.com (I.A. Abed).

http://dx.doi.org/10.1016/j.renene.2016.04.072
0960-1481/

Nomenclature

a	diode ideality factor
CR	crossover rate parameter
D	dimension of individual vector
d_i	deviation of RMSE for ith operational condition
F	mutation scaling parameter
F_{α}^{G}	resultant exerted force on α individual vector
$F_{\alpha\beta}^{G}$	exerted force on α individual vector by β vector
G	generation number
$G_1 - G_7$	seven operational condition (irradiance and cell temperature)
G_{max}	maximum generation number
I	current generated by the PV module (A)
I_e	experimental current generated by the PV module (A)
I_o	diode reverse saturation current (A)
I_p	computed current of the PV module (A)
I_{Ph}	photocurrent (A)
K	steepness of the logistic sigmoid curve
kB	Boltzmann's constant (1.3806503e−23 J/K)
l	random number in the range [1, D]
L	maximum value of the logistic sigmoid curve ($L = 1$)
m	number of solar radiation levels
M_d	mutation operation of DE algorithm
M_e	mutation operation of EM algorithm
n	length of the dataset
N	number of individual vectors in population set
q	electron charge (1.60217646e−19 C)
$q_{\alpha\beta}^{G}$	charge between α and β individual vectors
R	random number in the range [0, 1]
R_p	shunt resistance (Ω)
R_s	series resistance (Ω)
R^2	determination coefficient
S	population set
T_C	cell temperature (K)
V	voltage generated by the PV module (V)
V_e	experimental voltage generated by the PV module (V)
V_t	diode thermal voltage (V)
$X_{j,i}$	jth parameter of ith individual vector
$X_{j,L,i}$	lower limit of jth parameter of ith individual vector
$X_{j,H,i}$	upper limit of jth parameter of ith individual vector
X_i^G	ith individual vector in G generation (target vector)
$\widehat{X}_i^G$	mutant vector of ith individual vector in G generation
$y_{j,i}^G$	jth parameter of ith trial vector
ω_o	sigmoid midpoint on the x-axis ($\omega_o = 0$)
ε_1	switching control parameter of DEIM ($\varepsilon_1 \in [0, 1]$)
ε_2	switching control parameter of DEAM ($\varepsilon_2 \in [0, 1]$)
σ	standard deviation of the row vectors of S
AE	absolute error
ANN	artificial neural network
CPU	central processing unit
DC	direct current
DE	differential evolution
DEAM	differential evolution with adaptive mutation per iteration
DEIM	differential evolution with integrated mutation per iteration
EA	evolutionary algorithm
EM	electromagnetism-like
FL	fuzzy logic
GA	genetic algorithm
IADE	improved adaptive differential evolution
LM	Levenberg-Marquardt
MBE	mean bias error
NR	Newton Raphson
PDE	penalty based differential evolution
PSO	particle swarm optimization
RMSE	root mean square error
STD	standard test deviation

optimization (PSO) [13]. Hasanien [14] extracted the parameters of a single-diode model based on the shuffled frog leaping algorithm under various operating conditions using different PV modules. The parameters of a double-diode model for three different PV module technologies were calculated using GA, PSO, and differential evolution (DE) in Ref. [15]. Ishaque et al. concluded that DE was the best approach for extracting model parameters compared with other methods. This result was supported in Ref. [16], in which a penalty-based DE (PDE) algorithm was used to extract the parameters of a PV module. Based on the results obtained in Ref. [16], the proposed PDE rapidly converged with optimal PV parameter values compared with other methods such as GA, PSO, and simulated annealing algorithms.

According to [16], the conventional DE algorithm is reliable and efficient for estimating the parameters of a PV module model. However, the accuracy and convergence speed of the DE algorithm are based on the values of the control parameters of the algorithm. Therefore, an inappropriate selection of control parameters may lead to failure or extremely slow convergence toward optimal parameter values. Considering the aforementioned issue, several authors have attempted to improve the DE algorithm by proposing control strategies for the mutation scaling factor and crossover rate. Lian et al. [17] proposed an improved adaptive DE algorithm (IADE) to calculate five parameters of a PV module model. IADE is an improved DE with a strategy for adjusting the mutation scaling factor and crossover rate. The results of [17] showed that IADE offered more accurate and rapid convergence than GA, PSO, and the original DE. In Ref. [18], Wenyin and Zhihua proposed an improved adaptive DE algorithm integrated with a crossover rate repairing technique and a ranking-based mutation (Rcr-IJADE) to extract the parameters of a PV module model. Their results showed that the Rcr-IJADE method offered higher accuracy and faster convergence than the conventional DE algorithm.

Motivated by the aforementioned issues, the effect of hybridizing the DE algorithm with other EAs, such as electromagnetism-like (EM) algorithms, on the accuracy of estimating the parameters of a PV module model is investigated in this study. Moreover, the influence of controlling the parameters of this hybrid algorithm on its efficiency is discussed. The proposed algorithms are improved versions of DE, namely, the DE algorithm with integrated mutation per iteration (DEIM) and the DE algorithm with adaptive mutation per iteration (DEAM). The proposed approaches are validated using experimental data and previously proposed algorithms such as PDE (which is similar to conventional DE) [16], IADE [17], and Rcr-IJADE [18].

2. PV module model

A solar cell can be modeled using a method called single-diode model. The photocurrent of a solar cell is represented by an ideal dependent current source that generates current according to solar radiation and ambient temperature. Meanwhile, a diode in reverse mode can be used to represent the output voltage of a solar cell. A large shunt resistance is used to express the saturation current of a diode, whereas a small series resistance is used to express the internal loss of a solar cell. The single-diode model electric circuit is shown in Fig. 1. The output current of a solar cell can be expressed by

$$I = I_{Ph} - I_o\left[\exp\left(\frac{V + IR_s}{V_t}\right) - 1\right] - \frac{V + IR_s}{R_p}, \tag{1}$$

where I and V are the output current and voltage, respectively; I_{Ph} is the photocurrent; I_o is the diode saturation current; R_s is the series resistance (Ω); R_p is the parallel resistance (Ω) and V_t is the diode thermal voltage, which can be given by

$$V_t = \frac{aKBT_C}{q}. \tag{2}$$

where q is the electron charge (1.60217646e−19 C); KB is the Boltzmann's constant (1.3806503e−23 J/K); T_C is the cell temperature (K); and a is the diode ideality factor that represents the components of diffusion and recombination currents.

However, other researchers have proposed a modified model by adding one more diode parallel to the first one; this model is called the two-diode model [19]. A new diode is added to consider the effect of charge carrier recombination. However, the two-diode model is more complex than the single-diode model. Therefore, the single-diode model is still preferred because of its satisfactory accuracy and simplicity [4,15], and thus, is used in this research. Villalva et al. [7] and Tao et al. [8] proposed a PV model by computing several model parameters that were directly based on weather conditions, whereas other parameters, such as a and R_s, were assumed constant. However, this procedure did not provide optimal values for model parameters, and consequently, the accuracy of the predicted I–V curve obtained using this method was questionable. Lim et al. [20] proposed an extensive computations method to identify the five parameters of single diode model based on a single I–V curve and reducing the parameter space from five to one. The proposed method in Ref. [20] deals with the diode model as a dynamic system. In the current work, all the five parameters of the single-diode model are simultaneously extracted to obtain optimal parameters, which consequently results in the accurate prediction of I–V curves.

2.1. Optimizing the parameters of a PV module model

Based on (1) and (2), the parameters that dominate the performance of the PV module are clearly I_{Ph}, I_o, R_s, R_p, and a. These parameters are unknown and sensitive to solar radiation and cell temperature. Therefore, an optimization algorithm can be used to obtain optimal parameter values. In this research, the root-mean-square error (*RMSE*) between the experimental and computed photovoltaic currents is used to formulate the objective function as follows:

$$f(\theta) = \sqrt{\frac{1}{n}\sum_{i=1}^{N} P(V_e, I_e, \theta)^2}, \tag{3}$$

where

$$P(V_e, I_e, \theta) = I_e - I_{ph} + I_o\left[\exp\left(\frac{V_e + I_pR_s}{V_t}\right) - 1\right] + \frac{V_e + I_pR_s}{R_p}, \tag{4}$$

where V_e and I_e are the experimental values of the voltage and the current, respectively; θ is the vector of the five parameters [I_{Ph}, I_o, R_s, R_p, a] that is optimized by the proposed method; and n is the length of the data set. The *RMSE* is a better criterion for evaluating the deviation of the estimated values from the real data over n data set than other statistical methods, such as absolute error (*AE*) and relative error [16,17]. Given that no information on the optimal values of the extracted parameters is available, we decrease the objective function, as described in (3), which leads to the optimal solution for the optimization problem.

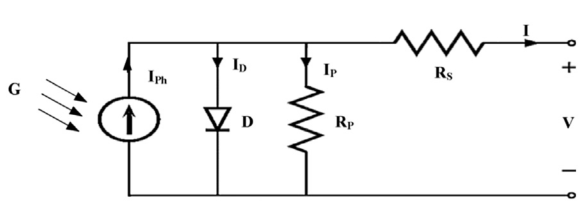

Fig. 1. Single-diode solar cell electrical equivalent circuit.

3. EAs for optimizing the parameters of a PV module model

In this study, different EAs are utilized to model a PV module. All these algorithms are population-based direct search algorithms that use an initial population set S and consist of randomly selected N D-dimensional individual vectors. A contraction process is used to drive these individual vectors toward optimal values to satisfy global minimization. The main mechanism of the attraction process is to replace bad individual vectors in population S with better individual vectors per iteration. For brevity, the mechanisms of EM and DE algorithms have not been explained in this paper; however, they are discussed in detail in Refs. [21] and [22], respectively. Efforts are devoted to discuss two new versions of hybrid DE–EM algorithms, namely, DEIM and DEAM. The main difference between these versions and the conventional DE algorithm lies in the mutation phase. The attraction–repulsion concept of the EM algorithm is used in DE to improve mutation operation. Mixed mutation concepts are used in these new versions. The first mutation concept is the classical mutation of the DE algorithm, which is denoted by M_d. The second mutation concept is the mutation operation used in the EM algorithm, which is denoted by M_e. The benefit of hybrid mutation is the capability to investigate reliability (optimal solution accuracy) and efficiency (CPU execution time and the number of evaluations of the objective function) [23]. Fig. 2 shows the proposed method to extract the parameters of PV module using EM algorithm.

3.1. DEIM

DEIM is similar to other population-based direct search algorithms that use N D-dimensional vectors as a population set (S) to search for the optimal parameters in the search space. The population set is defined as

$$S^G = \left[X_1^G, X_2^G, \ldots\ldots, X_N^G\right] = \left[X_i^G\right], \tag{5}$$

where

$$X_i = \left[X_{1,i}, X_{2,i}, \ldots\ldots, X_{D,i}\right] = \left[X_{j,i}\right], \tag{6}$$

where X_i is the target vector, i is the number of individuals (candidate solutions) of the population (i = 1, 2,……, N), j is the

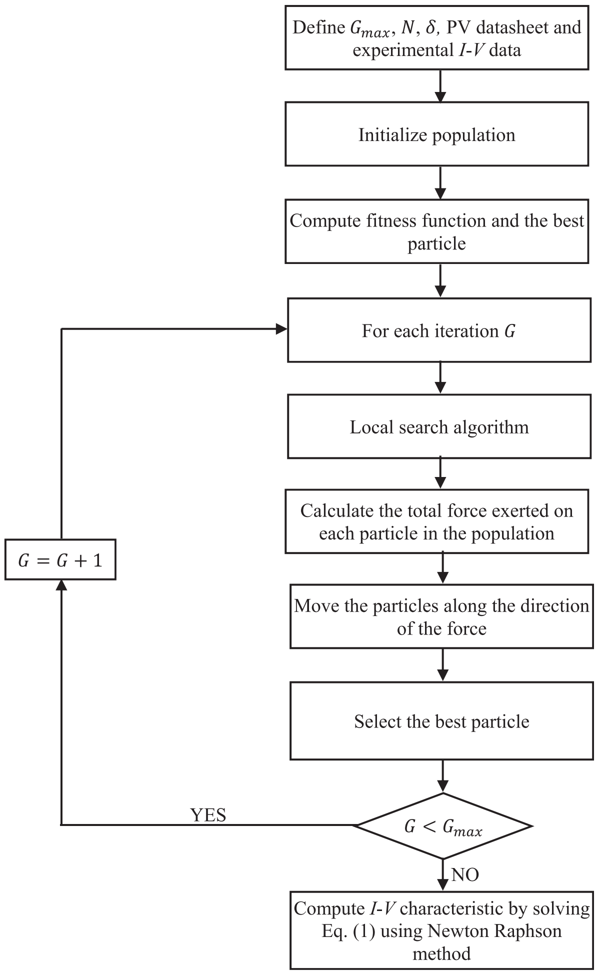

Fig. 2. Flow chart of estimating PV module's parameters based on EM algorithm.

dimension of the individual vector ($j = 1, 2, \ldots\ldots, D$), and G is the generation index ($G = 1, 2, \ldots\ldots, G_{max}$).

3.1.1. Initialization

The optimization process begins by creating an initial population $S^G = [X_i^G]$, where $G = 0$. The initial values of D parameters are selected randomly and distributed uniformly in the search region. The search region is limited by the lower and upper boundaries, which are defined as $X_{j,L}$ and $X_{j,H}$, respectively. The initial individual vector is selected based on the following:

$$X_{j,i}^0 = X_{j,L,i} + rand\left(X_{j,H,i} - X_{j,L,i}\right), \tag{7}$$

where *rand* is a random number within the [0, 1] interval.

3.1.2. Mutation

DEIM invokes both M_d and M_e operations in the same iteration [24]. The criterion adopted to use either M_d or M_e operation is as follows:

$$Mutation\ \ operation = \begin{cases} M_e & if\ \ \sigma_l^G < \varepsilon_1 \sigma_l^0 \\ M_d & otherwise \end{cases}, \tag{8}$$

where σ_l^G and σ_l^0 are elements of the vectors that represent the standard deviation of the row vectors of population S for G and initial generation, respectively; l is a randomly chosen number from the range [1, D]; and ε_1 is a constant parameter that controls the frequency of using M_e operation, that is, $\varepsilon_1 \in [0,1]$. Notably, the vector $\sigma^G = [\sigma_1^G, \sigma_2^G, \ldots\ldots, \sigma_D^G] = [\sigma_j^G]$, where $j = 1, 2, \ldots, D$, is computed at the beginning of each generation process. The mutant vector $\widehat{X}_i^G$, which is generated according to M_d operation, is described as follows:

$$\widehat{X}_i^G = X_\alpha^G + F\left(X_\beta^G - X_\gamma^G\right), \tag{9}$$

where X_α^G, X_β^G, and X_γ^G vectors are randomly selected from the population; and α, β, and γ are distinct indices that belong to the range [1, N]. The vector X_α^G is called the base vector, and F is a mutation scaling control parameter that is typically chosen within the [0.5, 1] interval.

Meanwhile, M_e mutation operation is also based on three distinct individual vectors that are randomly chosen from the population. However, unlike M_d, the index of one of these vectors may be the same index of the current target vector. M_e operation uses the total force exerted on one vector, namely, X_α^G by the other two vectors, namely, X_β^G and X_γ^G. Similar to the EM algorithm, the force exerted on X_α^G by X_β^G and X_γ^G is computed based on the charges between the vectors as follows:

$$q_{\alpha\beta}^G = \frac{f\left(X_\alpha^G\right) - f\left(X_\beta^G\right)}{f\left(X_w^G\right) - f\left(X_b^G\right)}, \tag{10}$$

$$q_{\alpha\gamma}^G = \frac{f\left(X_\alpha^G\right) - f\left(X_\gamma^G\right)}{f\left(X_w^G\right) - f\left(X_b^G\right)}, \tag{11}$$

where $f(X)$ is the objective function value for individual vector X; X_b^G and X_w^G are the best and worst individual vectors that represent the best and worst objective function values for the Gth generation, respectively; and G is the index that refers to the number of generation ($G = 1, 2, \ldots G_{max}$). The force exerted on X_α^G by X_β^G and X_γ^G are computed by

$$F_{\alpha\beta}^G = \left(X_\beta^G - X_\alpha^G\right) q_{\alpha\beta}^G, \tag{12}$$

$$F_{\alpha\gamma}^G = \left(X_\gamma^G - X_\alpha^G\right) q_{\alpha\gamma}^G. \tag{13}$$

Then, the resultant force exerted on X_α^G by X_β^G and X_γ^G is computed by

$$F_\alpha^G = F_{\alpha\beta}^G + F_{\alpha\gamma}^G. \tag{14}$$

Afterward, the mutant vector of M_e operation is computed as follows:

$$\widehat{X}_i^G = X_\alpha^G + F_\alpha^G. \tag{15}$$

3.1.3. Crossover

In this step, both the target vector X_i^G and the mutant vector $\widehat{X}_i^G$ are used to generate a trial vector $y_{j,i}^G$ as follows:

$$y_{j,i}^G = \begin{cases} \widehat{X}_{j,i}^G & if\ \ rand \le CR\ \ or\ \ j = I_i \\ X_{j,i}^G & \qquad otherwise \end{cases}, \tag{16}$$

where *rand* is a random number within the range of (0, 1), I_i is randomly selected index from the range of [1, D], and $CR \in [0,1]$ is the crossover control parameter. In this study, the trial vector is equal to the mutant vector when $CR = 1$.

The parameters of the trial vector should be checked to determine if they are lying outside the allowable search space to ensure that the parameter values are physical values. If a parameter exceeds the allowable limits of the search space, then it will be replaced with a new value as follows:

$$y_{j,i}^{G} = X_{j,L,i} + rand\left(X_{j,H,i} - X_{j,L,i}\right). \tag{17}$$

3.1.4. Selection

The selection step is applied after generating N trial vectors. The selection process between the current target vector and the trial vector is based on the objective function values of both vectors. The vector with a small objective function is chosen as a member of the population for the next generation $G + 1$. The selection process can be described as

$$X_i^{G+1} = \begin{cases} y_i^G & \text{if } f\left(y_i^G\right) < f\left(X_i^G\right) \\ X_i^G & \text{otherwise} \end{cases}. \tag{18}$$

The reproduction of trail vector (i.e., mutation and crossover) and selection stages continue until the predefined stopping conditions are satisfied. The pseudo code of DEIM algorithm is illustrated in Appendix A. In the meanwhile, the methodology of extracting the five parameters of a single-diode PV module model based on the DEIM algorithm is shown in Fig. 3.

3.2. DEAM

DEAM is similar to DEIM; however, it invokes either M_d or M_e operation along the iteration. The criterion used to switch between both types of mutation is as follows:

$$Mutation\ \ operation = \begin{cases} M_e & \text{if } \left\|\sigma^G\right\| < \varepsilon_2 \left\|\sigma^0\right\| \\ M_d & \text{otherwise} \end{cases}, \tag{19}$$

where σ^G and σ^0 are the norms of the vectors of the standard deviation of the row vectors of population S for G and initial generation, respectively; and ε_2 is a switching parameter used to switch between M_d and M_e operations, that is, $\varepsilon_2 \in [0,1]$. Fig. 4 shows the proposed DEAM algorithm for extracting the parameters of a single-diode PV module model.

3.3. Proposed strategy for adapting the mutation scaling factor and crossover rate in DEIM and DEAM

The mutation scaling factor (F) and crossover rate (CR) are fixed in the original DE algorithm. When F and CR control parameters are fixed with inappropriate values, DE may sometimes fail to converge to the global minimizer. Therefore, the performance of the DE algorithm is based on how F and CR are selected. However, finding the optimal control parameters of DE through trial-and-error is difficult, particularly when equilibrium between efficiency and reliability is required.

Different strategies have been proposed in Refs. [25–28] to adjust the control parameters within the search process. These strategies provide accurate global optimal results, but require complex computations. Thus, the feasibility of these strategies is questionable for the off-line optimization process and high-dimensional optimization problems. Lian et al. [17] proposed a simple method to adjust the control parameters of DE. This method

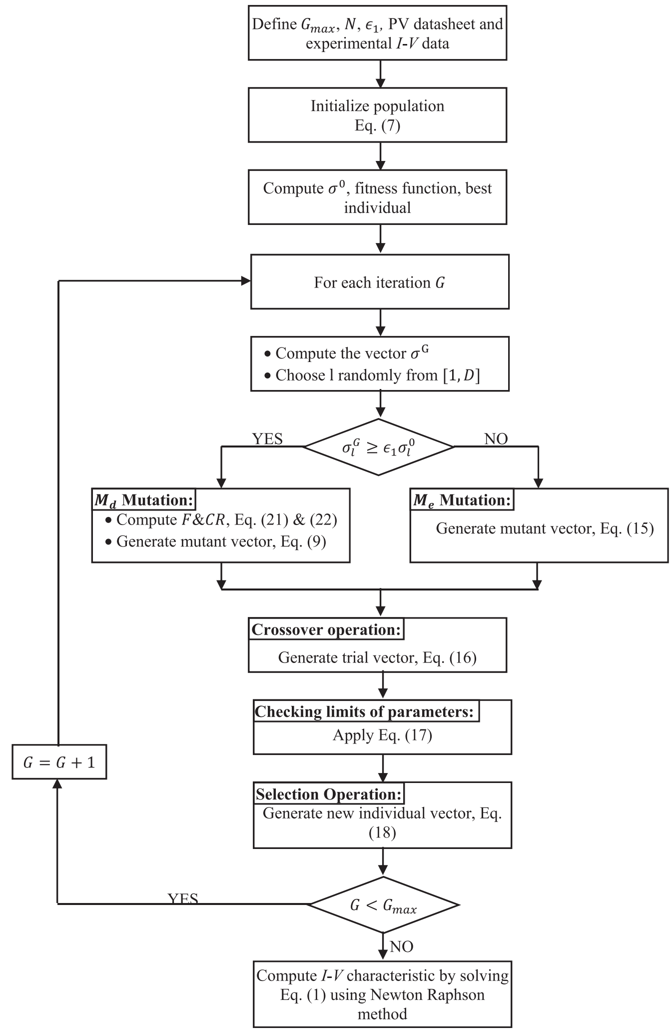

Fig. 3. Flow chart of the proposed DEIM algorithm for extracting parameters of PV module.

was based on the exponent of the random weighted ratio of the current and previous best objective function values to adapt control parameters within the range of [0.5, 1]. Furthermore, Kaelo [23] used a random control parameter per iteration, where F was randomly selected from the range of [0.4, 1], whereas CR was randomly chosen from the range of [0.5, 0.7]. According to [22], the control parameter values outside the range of [0.4, 1] were less effective. Therefore, a simple and accurate method is proposed in this paper to adjust the control parameters per iteration within [0.5, 1] period. A logistic sigmoid function is used as follows:

$$g(x) = \frac{L}{1 + \exp(-K(\omega - \omega_o))}, \tag{20}$$

where ω_o is the sigmoid midpoint on the x-axis ($\omega_o = 0$), L is the maximum value of the curve ($L = 1$), and K is the steepness of the curve. Parameter ω in (20) is the difference between the best objective function values for the current and previous generations weighted by a random number as described below:

$$\omega = \left[f\left(X_{best}^G\right) - f\left(X_{best}^{G-1}\right)\right] * rand, \tag{21}$$

where X_{best}^G and X_{best}^{G-1} are the best individual vectors for G and $G - 1$

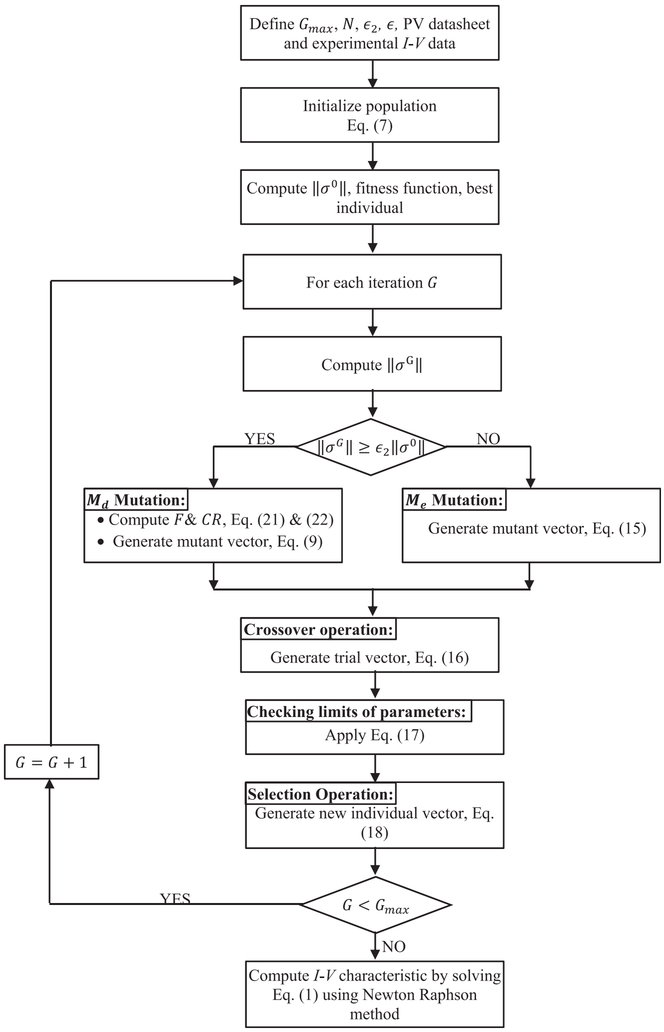

Fig. 4. Flow chart of estimating PV module's parameters based on DEAM algorithm.

generations, respectively, and *rand* is a randomly selected number from the range of [0, 1]. The expressions for F and CR are alike because the ranges of these values are similar. The expression of F and CR is given as follows:

$$F, CR = A\left(\frac{L}{1+\exp(-K(\omega-\omega_o))}+B\right), \tag{22}$$

where A and B constants are selected to enable F and CR to remain within the range of [0.5, 1], $A = 0.5$ and $B = 1$.

3.4. Evaluation criteria of the proposed algorithms

Six statistical values are used in this study to evaluate the proposed algorithms. These statistical values are absolute error (*AE*), root mean square error (*RMSE*), mean bias error (*MBE*), coefficient of determination (R^2), deviation of *RMSE* for each solar radiation level (d_i) and standard test deviation of *RMSE* (*STD*).

AE can be defined as the absolute difference between the computed and experimental currents for a given voltage point under a specific solar radiation and cell temperature as follows:

$$AE = |I_p - I_e|, \tag{23}$$

where I_e and I_p are the experimental and computed currents, respectively.

Meanwhile, *RMSE* is a statistical indicator that refers to the standard deviation between the computed and experimental data of a sample of n data points. *RMSE* measures unsystematic error and is defined as

$$RMSE = \sqrt{\frac{1}{n}\sum_{i=1}^{n}\left(I_p - I_e\right)^2}, \tag{24}$$

where n is the number of I–V data points.

Another statistical indicator, *MBE*, is used to measure the performance of the proposed model. *MBE* is a measure of systematic error (overall bias error) and can be defined as

$$MBE = \frac{1}{n}\left(\sum_{i=1}^{n}\left(I_p - I_e\right)\right). \tag{25}$$

By contrast, R^2 is used to evaluate the performance and accuracy of the proposed model. It reflects the degree to which the proposed model follows the variation in the experimental data. The preferred value of R^2 must be close to 1. R^2 is calculated by

$$R^2 = 1 - \frac{\sum_{i=1}^{n}\left(I_p - I_e\right)^2}{\sum_{i=1}^{n}\left(I_e - \overline{I_e}\right)^2}, \tag{26}$$

where $\overline{I_e}$ is the arithmetic mean of the experimental current ($\overline{I_e} = \frac{1}{n}\sum_{i=1}^{n} I_e$).

The deviation of *RMSE* for each solar radiation level measures the deviation of a particular *RMSE* for a given solar radiation level from the mean *RMSE* value for all solar radiation levels. The d_i value shows the capability of a method to estimate optimal parameters with respect to the solar radiation level. d_i is calculated by

$$d_i = RMSE_i - \overline{RMSE}, \tag{27}$$

where $\overline{RMSE}$ is the arithmetic mean of the *RMSE* value for all solar radiation levels ($\overline{RMSE} = \frac{1}{m}\sum_{i=1}^{m} RMSE$), m is the total number of solar radiation levels, and i is a particular solar radiation level ($i = 1, 2, \ldots, m$).

The last statistical value used to evaluate the results of the proposed models is the standard test deviation (*STD*) of *RMSE*. This value shows the deviation in *RMSE* of the proposed model for n tests. *STD* is given by

$$STD = \sqrt{\frac{1}{(n-1)}\sum_{i=1}^{n} d_i^2}. \tag{28}$$

The proposed method is based on experimental data for the I–V curves to determine the optimal values of the parameters. Thus, the utilized I–V curve data should be obtained for most of the I–V curve regions. Therefore, using a large and well-distributed data set improves fitting between the computed and measured I–V curves.

4. Results and discussion

A Kyocera KC120-1 multi-crystalline 120 Wp PV module was used in this work. The targeted data were derived from experimental characterization of the PV module. The adopted PV module was installed at a solar structure at the University Kebangsaan Malaysia, Malaysia. Data were extracted by using a DC–DC converter-based I–V characteristic generator. The accuracy of the utilized I–V characteristic generator was approximately 99%–99.5%. In this research, EM, DEIM, and DEAM were adopted to

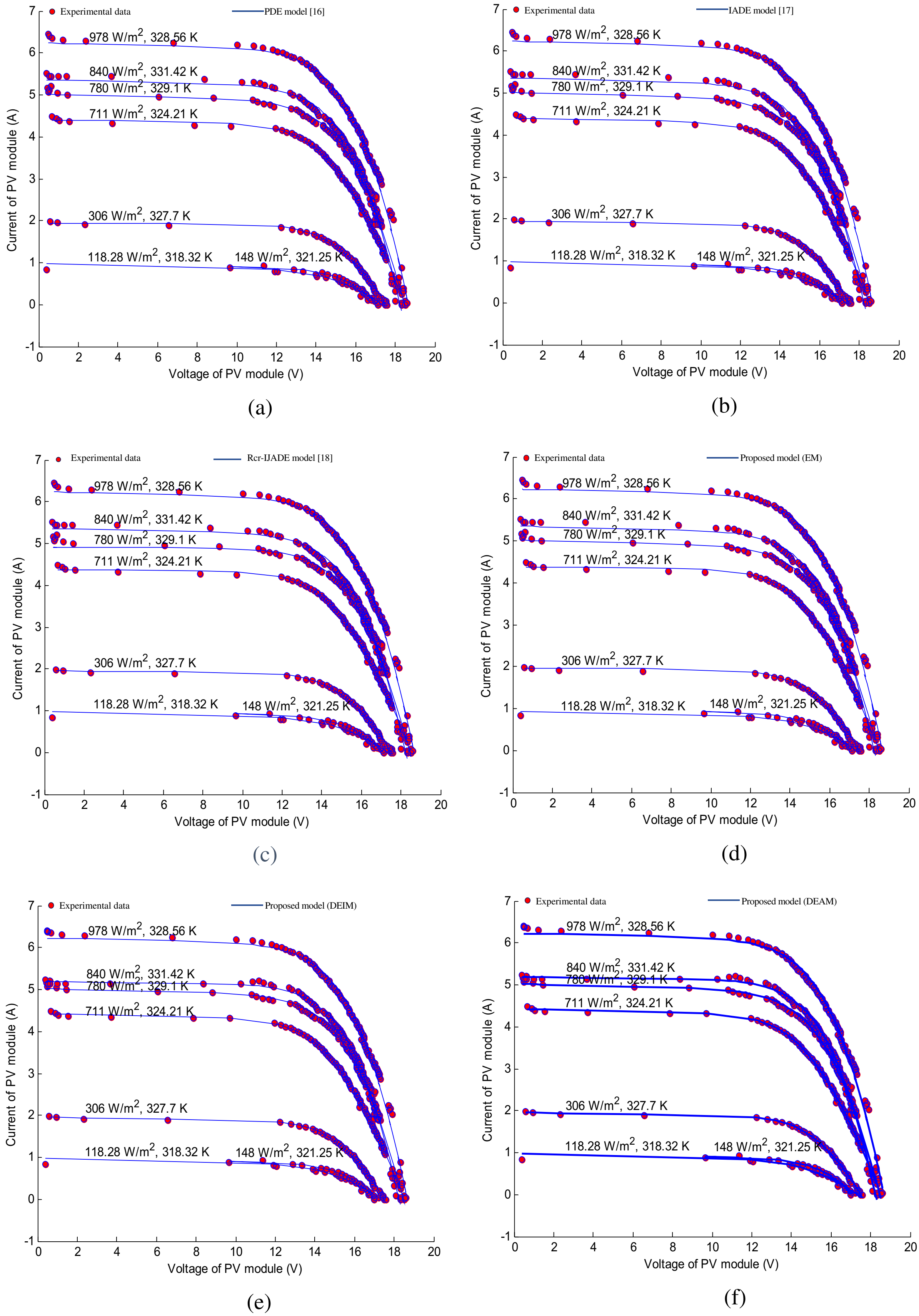

Fig. 5. *I-V* characteristics of PV module under different weather condition using various evolutionary algorithms (a) PDE, (b) IADE, (c) Rcr-IJADE, (d) EM, (e) DEIM and (f) DEAM.

Table 1
Predicted parameters of the selected PV module by various evolutionary algorithms.

Parameter	Method	G1	G2	G3	G4	G5	G6	G7	Average
a	PDE	1.326	1.362	1.186	1.301	1.381	1.348	1.375	1.326
	IADE	1.193	1.225	1.085	1.213	1.381	1.348	1.375	1.260
	Rcr-IJADE	1.401	1.338	1.295	1.287	1.356	1.345	1.376	1.343
	EM	1.508	1.401	1.359	1.290	1.380	1.317	1.363	1.374
	DEIM	1.123	1.241	1.091	1.216	1.381	1.350	1.376	1.254
	DEAM	1.133	1.230	1.074	1.207	1.381	1.350	1.376	1.250
R_s	PDE	1.551	0.380	0.727	0.525	0.266	0.209	0.215	0.553
	IADE	1.789	0.571	0.762	0.548	0.266	0.209	0.215	0.623
	Rcr-IJADE	1.428	0.418	0.647	0.533	0.273	0.205	0.217	0.532
	EM	1.181	0.395	0.592	0.530	0.266	0.220	0.218	0.486
	DEIM	1.920	0.425	0.714	0.552	0.270	0.198	0.217	0.614
	DEAM	1.905	0.439	0.730	0.553	0.270	0.198	0.217	0.616
R_p	PDE	100.2	125.2	1868.1	209.9	100.0	100.0	100.0	371.9
	IADE	100.0	117.8	245.8	120.0	100.0	100.0	100.0	126.2
	Rcr-IJADE	100.1	129.7	4592.2	361.9	503.1	100.9	100.7	841.2
	EM	183.9	139.2	5000.0	403.1	100.0	100.0	100.0	860.9
	DEIM	100.0	114.6	187.3	119.7	100.0	309.1	100.0	147.3
	DEAM	100.0	114.0	181.4	115.2	100.0	309.1	100.0	145.7
I_{ph}	PDE	1.000	1.002	1.937	4.412	5.031	5.373	6.249	3.572
	IADE	1.000	1.001	1.954	4.426	5.031	5.373	6.249	3.576
	Rcr-IJADE	1.000	1.001	1.948	4.385	4.916	5.374	6.250	3.554
	EM	0.929	1.000	1.952	4.386	5.031	5.364	6.247	3.559
	DEIM	1.000	1.000	1.965	4.441	5.037	5.186	6.246	3.554
	DEAM	1.000	1.000	1.965	4.441	5.037	5.186	6.246	3.554
I_o	PDE	1.5E-6	2.9E-6	9.3E-7	3.1E-6	1.0E-5	1.0E-5	1.0E-5	5.5E-6
	IADE	3.3E-7	7.1E-7	2.4E-7	1.1E-6	1.0E-5	1.0E-5	1.0E-5	4.6E-6
	Rcr-IJADE	3.0E-6	2.4E-6	3.2E-6	2.7E-6	8.0E-6	9.8E-6	1.0E-5	5.6E-6
	EM	7.4E-6	4.2E-6	6.0E-6	2.8E-6	9.9E-6	7.3E-6	8.9E-6	6.7E-6
	DEIM	1.3E-7	8.7E-7	2.6E-7	1.1E-6	1.0E-5	1.0E-5	1.0E-5	4.6E-6
	DEAM	1.5E-7	7.7E-7	2.0E-7	1.0E-6	1.0E-5	1.0E-5	1.0E-5	4.6E-6

Table 2
RMSE, MBE, R^2 and CPU-execution time of various methods under various weather conditions.

Tool	Method	G1	G2	G3	G4	G5	G6	G7	Average
RMSE	PDE	0.054	0.018	0.035	0.038	0.105	0.110	0.148	0.072
	IADE	0.053	0.017	0.034	0.037	0.105	0.110	0.148	0.073
	Rcr-IJADE	0.054	0.018	0.036	0.038	0.114	0.111	0.148	0.074
	EM	0.047	0.019	0.037	0.038	0.105	0.112	0.149	0.073
	DEIM	0.046	0.014	0.026	0.028	0.095	0.088	0.136	0.062
	DEAM	0.046	0.014	0.026	0.028	0.095	0.088	0.136	0.062
MBE	PDE	0.003	0.000	0.001	0.001	0.011	0.012	0.022	0.007
	IADE	0.003	0.000	0.001	0.001	0.011	0.012	0.022	0.007
	Rcr-IJADE	0.003	0.000	0.001	0.001	0.013	0.012	0.022	0.008
	EM	0.002	0.000	0.001	0.001	0.011	0.013	0.022	0.007
	DEIM	0.002	0.000	0.001	0.001	0.009	0.008	0.019	0.006
	DEAM	0.002	0.000	0.001	0.001	0.009	0.008	0.019	0.006
R^2	PDE	0.956	0.996	0.997	0.999	0.993	0.993	0.991	0.989
	IADE	0.957	0.996	0.997	0.999	0.993	0.993	0.991	0.989
	Rcr-IJADE	0.956	0.996	0.996	0.999	0.992	0.993	0.991	0.989
	EM	0.966	0.996	0.996	0.999	0.993	0.993	0.991	0.990
	DEIM	0.967	0.998	0.998	0.999	0.994	0.996	0.992	0.992
	DEAM	0.967	0.998	0.998	0.999	0.994	0.996	0.992	0.992
CPU-execution time	PDE	19.88	18.71	19.88	21.29	20.59	21.67	21.11	20.32
	IADE	19.64	18.74	20.39	20.89	20.14	21.23	21.23	20.45
	Rcr-IJADE	18.92	18.88	19.58	20.86	20.65	21.01	21.04	20.14
	EM	2465	2412	2471	2677	2448	2585	2588	2521
	DEIM	18.91	17.63	18.25	19.45	19.56	19.88	19.52	19.03
	DEAM	17.16	17.36	17.93	19.41	19.50	19.38	19.45	18.60

extract the parameters of a single-diode PV module model. Results of DE [16], IADE [17], and Rcr-IJADE [18] were obtained from previous research. The search areas for a, R_s, R_p, I_{ph}, and I_o were assumed to be within the ranges of [1,2], [0.1, 2] Ω, [100, 5000] Ω [1,8], A, and [1e−12,1e−5] A, respectively [7,16]. The maximum number of iteration was set to 500 and selected population size was 10 D for all algorithms. After conducting extensive experiments on all algorithms, changes in the objective function values were determined to be insignificant after 500 iterations. Finally, accuracy of the proposed approaches was verified by comparing the obtained results with real experimental data.

According to [16], we set mutation scaling factor (F) and crossover rate (CR) in the PDE algorithm (conventional DE) 0.8 and 1.0, respectively. Meanwhile, F and CR parameters were adaptive for each iteration in IADE. For DEAM and DEIM, F and CR parameters were tuned for each individual vector processing per iteration. In this study, ε_1 and ε_2 were set to 0.28 and 0.23, respectively, to provide improved results after several attempts. Fig. 5a–f showed

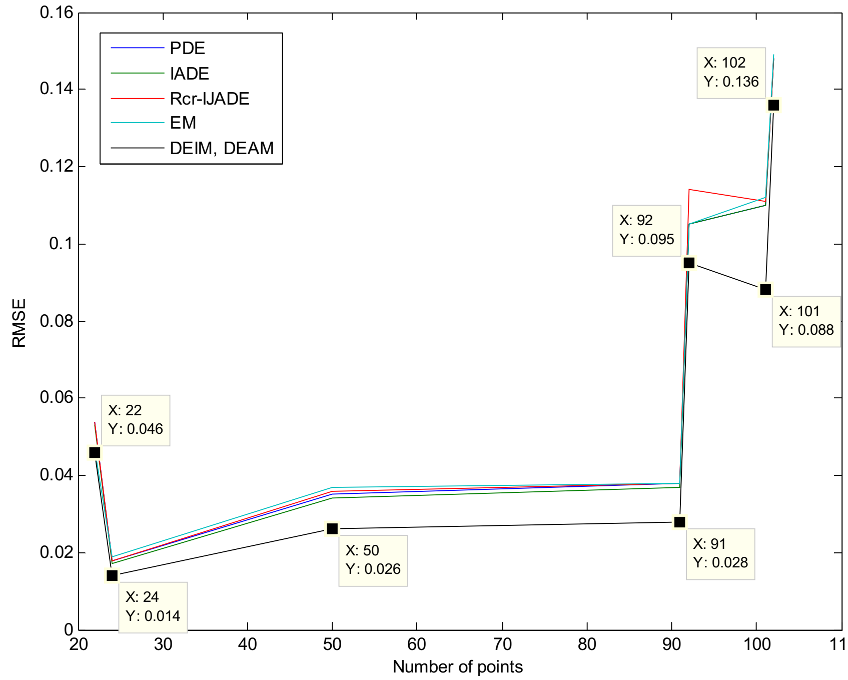

Fig. 6. RMSE of PDE, IADE, Rcr-IJADE, EM, DEIM and DEAM algorithms with respect to number of *I-V* data points under different weather conditions.

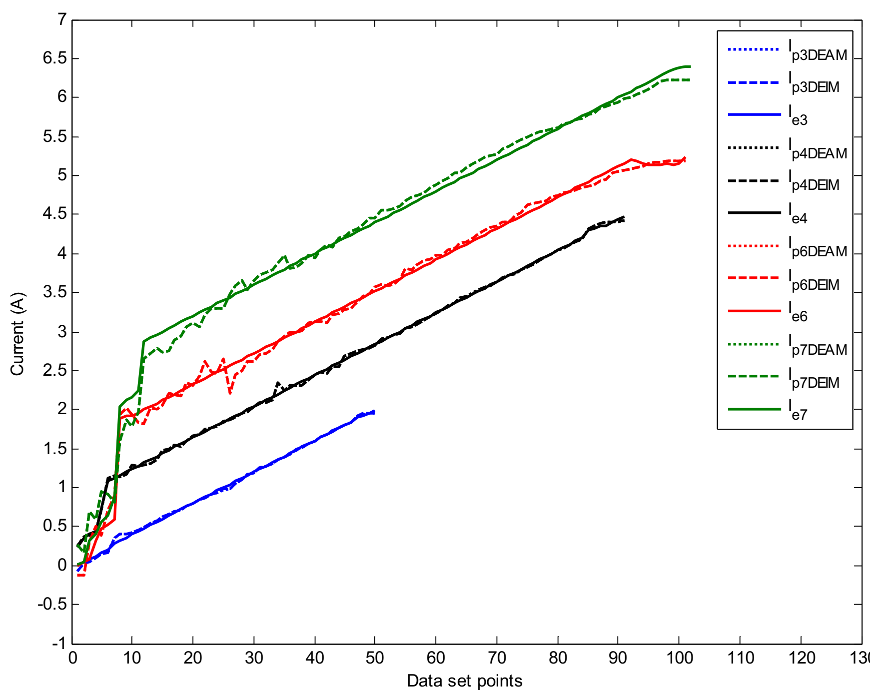

Fig. 7. Experimental and computed values of current based on DEAM and DEIM algorithms versus data set points.

I–V characteristic curves for the adopted PV module based on extracted parameters using PDE, IADE, Rcr-IJADE, EM, DEIM, and DEAM.

Table 1 presents the average values of predicted parameters of the PV module that were extracted by using PDE, IADE, Rcr-IJADE, EM, DEIM, and DEAM. The parameters estimated by DEIM and DEAM were equal for G5–G7 operation conditions. The parameters estimated by PDE were similar to the values estimated by IADE for G5–G7 operation conditions. The *a* parameter of all the algorithms were acceptable and within the range of [1, 1.4]. The R_s, I_{ph}, and I_o extracted by all the algorithms are within the ranges of [0.2, 1.9], [0.9, 6.3], [1.3e−7, 1e−5], respectively.

Based on Fig. 5, all the algorithms successfully predicted the I–V curves. However, to study the performance of these algorithms in detail, comparison in terms of *AE*, *RMSE*, *MBE*, R^2, d_i, and *STD* was conducted. Table 2 shows the results of the comparison in terms of *RMSE*, *MBE*, and CPU execution time of the proposed models under various weather conditions. The results showed DEAM- and DEIM-

Table 3
d_i and STD of various methods under various weather conditions.

Solar radiation	PDE	IADE	Rcr-IJADE	EM	DEIM	DEAM
G1	−0.01904	−0.01882	−0.02047	−0.02510	−0.01556	−0.01553
G2	−0.05440	−0.05489	−0.05623	−0.05385	−0.04825	−0.04823
G3	−0.03775	−0.03852	−0.03812	−0.03544	−0.03597	−0.03610
G4	−0.03493	−0.03553	−0.03635	−0.03469	−0.03389	−0.03389
G5	0.03263	0.03317	0.04031	0.03269	0.03310	0.03313
G6	0.03791	0.03845	0.03678	0.03984	0.02628	0.02630
G7	0.07558	0.07613	0.07408	0.07655	0.07430	0.07432
STD	0.00236	0.00241	0.00247	0.00242	0.00205	0.00206

Table 4
Performance of various algorithms for five-parameter estimation with experimental data under different weather conditions.

Solar radiation	Fitness value	PDE	IADE	Rcr-IJADE	EM	DEIM	DEAM
G1	Maximum	0.28963	0.34639	0.20247	0.39097	0.24912	0.34862
	Minimum	0.05349	0.05317	0.05371	0.04738	0.0464	0.0464
	Average	0.05861	0.05883	0.05575	0.04945	0.05007	0.04965
G2	Maximum	0.50404	0.42046	0.17184	0.31271	0.12696	0.10708
	Minimum	0.01813	0.0171	0.01795	0.01863	0.01371	0.01371
	Average	0.0243	0.02408	0.02377	0.03311	0.01632	0.016
G3	Maximum	0.14225	0.4557	0.18785	0.40918	0.10314	0.13792
	Minimum	0.03478	0.03346	0.03606	0.03704	0.02599	0.02583
	Average	0.03815	0.03849	0.03776	0.05465	0.02896	0.02839
G4	Maximum	0.21688	0.41445	0.40215	0.51200	0.39264	0.10705
	Minimum	0.0376	0.03645	0.03782	0.03779	0.02808	0.02804
	Average	0.04707	0.04292	0.04275	0.20683	0.03275	0.03123
G5	Maximum	0.47755	0.59895	0.44704	0.58153	0.54221	0.59405
	Minimum	0.10516	0.10516	0.11448	0.10517	0.09506	0.09506
	Average	0.1156	0.11332	0.12334	0.26259	0.10205	0.10361
G6	Maximum	0.44513	0.37149	0.22971	0.35345	0.41446	0.64693
	Minimum	0.11044	0.11044	0.11095	0.11232	0.08824	0.08824
	Average	0.12115	0.11894	0.11849	0.14844	0.09249	0.09557
G7	Maximum	0.59269	0.67832	0.54344	0.73617	0.6453	0.42242
	Minimum	0.14811	0.14811	0.14825	0.14903	0.13626	0.13626
	Average	0.16044	0.15633	0.15723	0.22584	0.14124	0.14223
Mean value	Maximum	0.38117	0.46940	0.31207	0.28399	0.35340	0.33773
	Minimum	0.07253	0.07198	0.07417	0.07431	0.06196	0.06194
	Average	0.08076	0.07899	0.07987	0.08471	0.06627	0.06667

based models were more accurate compared with the other models. The average values of *RMSE* and *MBE* for the DEAM-based model were approximately 0.0619 A and 0.0056 A, respectively; whereas those for DEIM were approximately 0.062 A and 0.0056 A, respectively. Moreover, DEAM and DEIM yielded the highest R^2 value of approximately 0.9921. DEAM exhibited more rapid convergence with optimal parameter values than other algorithms when CPU execution time was approximately 18.6 s. Based on these results, the proposed adaptive mutation and control parameters (*F* and *CR*) per generation have assisted the algorithm to converge toward global optimal values.

The sensitivity of model output to the distribution and number of I–V data points cannot be specified because two other variables (i.e., solar irradiance and cell temperature) also affect sensitivity. Moreover, the proposed model is not a learning machine whose accuracy increases when data set size is increased. The objective function presented in this work is highly multi-modal and has noisy characteristics because of utilized experimental data. When the number of data points is increased, *RMSE* may increase, as shown in Fig. 6. Fig. 7 shows the correlations between the experimental and computed values of the current using DEAM and DEIM algorithms. Correlation is explained for four operation conditions (G3, G4, G6, and G7) to avoid overcrowding of traces. According to Fig. 7, the computed values of the current by both proposed algorithms are very close to the experimental values of current. However, the values of current calculated by DEAM and DEIM algorithms are very close to each other, and thus recognizing these values in one plot's area is difficult.

Furthermore, Table 3 presents the comparison of the proposed methods in terms of d_i and *STD*. DEAM and DEIM exhibited the lowest *STD* values of approximately 0.00206 and 0.00205, respectively, compared with those of other methods. Finally, Table 4 shows the fitness function values of different EAs under various weather conditions. DEIM and DEAM provided the lowest mean of average fitness function values at approximately 0.06627 and 0.06667, respectively, under all solar radiation levels. Moreover, the lowest mean of the minimum fitness function values were also achieved by DEAM and DEIM at approximately 0.06194 and 0.06196, respectively.

Fig. 8 shows convergence of the average of the instantaneous fitness function values of the proposed and other algorithms under various weather conditions. The average value of fitness functions of both DEIM and DEAM is 0.065 after 50 generations. By contrast, the average fitness function values of IADE [17], PDE [16], Rcr-IJADE [18], and EM after 500 generations are 0.072, 0.073, 0.074, and 0.078, respectively. Thus, both DEIM and DEAM offer better convergence toward optimal parameter values than the other algorithms. The first 50 generations in Fig. 8 are displayed in Fig. 9 for emphasis. The evolution of fitness function values of DEIM and DEAM algorithms is considerably faster than the other algorithms for the first 50 generations.

5. Conclusion

The five parameters of a single-diode PV module model were estimated by using various EAs, namely, EM and two improved

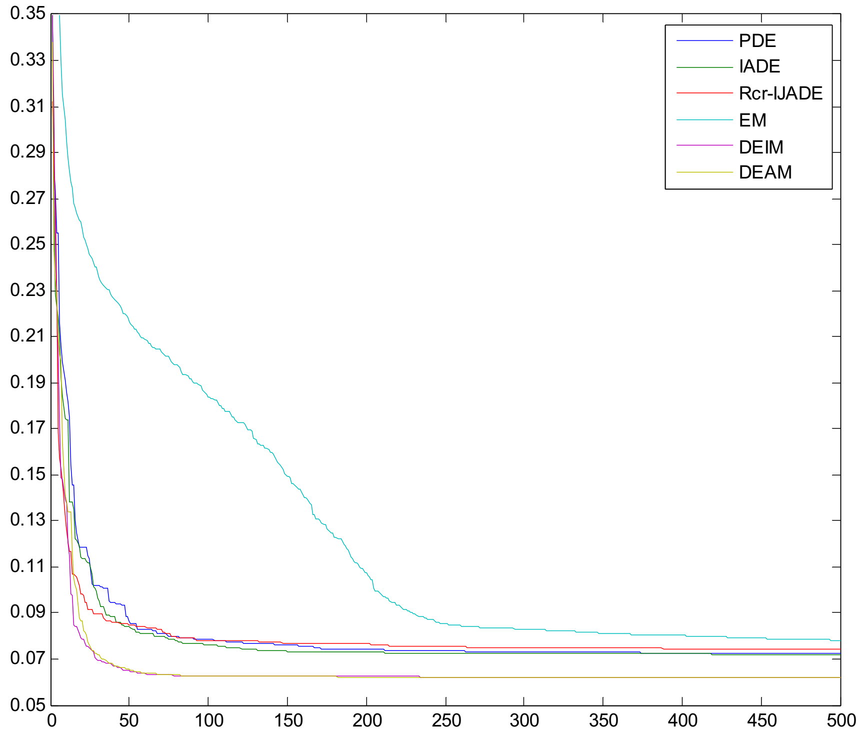

Fig. 8. Development of fitness function values of PDE, IADE, Rcr-IJADE, EM, DEIM and DEAM algorithms.

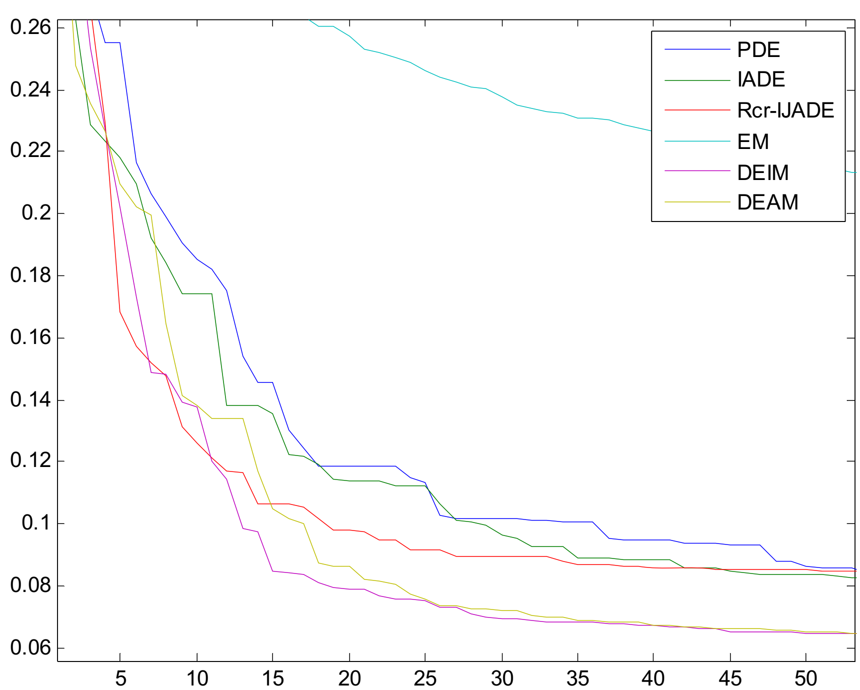

Fig. 9. Development of fitness function values of various algorithms for first 50 generations.

versions of the DE algorithm (i.e., DEIM and DEAM). The proposed DEIM and DEAM algorithms combined the attraction–repulsion mechanism of the EM algorithm with conventional DE algorithm to boost mutation operation. In addition, a simple adaptive method was used in DEIM and DEAM to tune the mutation-scaling factor and crossover rate per iteration based on a sigmoid function for the difference between fitness function values of current and previous iterations. The proposed methods were validated using real experimental data and previously methods. Results showed that the proposed DEIM and DEAM offered interesting advantages over the other methods, including high estimation accuracy, rapid convergence, and fewer control parameters.

Appendix A

Pseudo code of the DEIM algorithm

Initialization the algorithm;
Set parameter limits $[X_L, X_H]$, *population size* (N), *maximum number of generation* $(G_{max}), \epsilon_1, \epsilon$, *datasheet information of PV module, experimental I-V data of PV module*
Randomly generate initial population $X_{j,i}^0 = X_{j,L,i} + rand(X_{j,H,i} - X_{j,L,i})$
Compute $\|\sigma^0\|$
Set $G = 1$
$fitness\_best1 = min\left(f(X_i^0)\right)$
$fitness\_best2 = fitnes\_best1$
$fitness\_worst = max\left(f(X_i^0)\right)$
$X_{best} = X\left(min\left(f(X_i^0)\right)\right)$
While $(G \le G_{max})$ *and* $(fitness_{best1} > \epsilon)$

Generate mutation factor and crossover rate;
$\omega = [f(X_{best}^G) - f(X_{best}^{G-1})] * rand$
$F = A * (L/(1 + exp(-k * \omega)) + B)$
$CR = A * (L/(1 + exp(-k * \omega)) + B)$
for $i = 1$ *to* N
Randomly choose three distinct individual vectors X_α^G, X_β^G *and* X_γ^G *from the current population where* $X_\alpha^G \ne X_\beta^G \ne X_\gamma^G$

Choose l *randomly from the range [1, D]*
If $\sigma_l^G \ge \epsilon_1 \sigma_l^0$
M_d *Mutation step*
$\hat{X}_i^G = X_{best}^G + F(X_\beta^G - X_\gamma^G)$
else
M_e *Mutation steps*
$q_{\alpha\beta}^G = \left(f(X_\alpha^G) - f(X_\beta^G)\right)/(fitnes\_worst - fitness\_best1)$
$q_{\alpha\gamma}^G = \left(f(X_\alpha^G) - f(X_\gamma^G)\right)/(fitnes\_worst - fitness\_best1)$
$F_{\alpha\beta}^G = (X_\beta^G - X_\alpha^G)q_{\alpha\beta}^G$
$F_{\alpha\gamma}^G = (X_\gamma^G - X_\alpha^G)q_{\alpha\gamma}^G$
$F_\alpha^G = F_{\alpha\beta}^G + F_{\alpha\gamma}^G$
$X_i^G = X_\alpha^G + F_\alpha^G$
end if
Generate trail vector (Crossover);

Choose I_i *randomly from the range [1, D]*
for $j = 1$ *to* D
if $(rand \le CR)$ *or* $(j = I_i)$
$y_{j,i}^G = \hat{X}_{j,i}^G$
else
$y_{j,i}^G = X_{j,i}^G$

end if
end for
for $j = 1$ *to* D
if $(y_{j,i}^G < X_{j,L})$ *or* $(y_{j,i}^G > X_{j,H})$
$y_{j,i}^G = X_{j,L,i} + rand(X_{j,H,i} - X_{j,L,i})$
end if
end for
Generate new population (Selection);
if $f(y_i^G) < f(X_i^G)$
$X_i^{G+1} = y_i^G$
end if
end for
$fitness\_best2 = fitnes\_best1$
$fitness\_best1 = min\left(f(X_i^G)\right)$
$fitness\_worst = max\left(f(X_i^G)\right)$
$X_{best} = X\left(min\left(f(X_i^G)\right)\right)$

$G = G + 1$
end while

References

[1] M. Vafaeipour, S. Hashemkhani Zolfani, M.H. Morshed Varzandeh, A. Derakhti, M. Keshavarz Eshkalag, Assessment of regions priority for implementation of solar projects in Iran: new application of a hybrid multi-criteria decision making approach, Energy Convers. Manag. 86 (2014) 653–663.

[2] T. Khatib, W. Elmenreich, Novel simplified hourly energy flow models for photovoltaic power systems, Energy Convers. Manag. 79 (2014) 441–448.

[3] D. King, W. Boyson, J. Kratochvil, Photovoltaic Array Performance Model, Sandia National Laboratories, 2004 paper nr. SAND2004–3844.

[4] T. Ma, H. Yang, L. Lu, Solar photovoltaic system modeling and performance prediction, Renew. Sustain. Energy Rev. 36 (2014) 304–315.

[5] D.S.H. Chan, J.C.H. Phang, Analytical methods for the extraction of solar-cell single- and double-diode model parameters from I-V characteristics, Electron Devices IEEE Trans. 34 (1987) 286–293.

[6] G. Ciulla, V. Lo Brano, V. Di Dio, G. Cipriani, A comparison of different one-diode models for the representation of I–V characteristic of a PV cell, Renew. Sustain. Energy Rev. 32 (2014) 684–696.

[7] M.G. Villalva, J. R Gazoli, E. R Filho, Comprehensive approach to modeling and simulation of photovoltaic arrays, Power Electron. IEEE Trans. 24 (2009) 1198–1208.

[8] T. Ma, H. Yang, L. Lu, Development of a model to simulate the performance characteristics of crystalline silicon photovoltaic modules/strings/arrays, Sol. Energy 100 (2014) 31–41.

[9] M. Karamirad, M. Omid, R. Alimardani, H. Mousazadeh, S.N. Heidari, Ann based simulation and experimental verification of analytical four- and five-parameters models of PV modules, Simul. Model. Pract. Theory 34 (2013) 86–98.

[10] R.K. Kharb, S.L. Shimi, S. Chatterji, M.F. Ansari, Modeling of solar PV module and maximum power point tracking using ANFIS, Renew. Sustain. Energy Rev. 33 (2014) 602–612.

[11] M. Hejri, H. Mokhtari, M.R. Azizian, M. Ghandhari, L. Soder, On the parameter extraction of a five-parameter double-diode model of photovoltaic cells and modules, Photovolt. IEEE J. 4 (2014) 915–923.

[12] M.S. Ismail, M. Moghavvemi, T.M.I. Mahlia, Characterization of PV panel and global optimization of its model parameters using genetic algorithm, Energy Convers. Manag. 73 (2013) 10–25.

[13] V. Khanna, B.K. Das, D. Bisht, Vandana, P.K. Singh, A three diode model for industrial solar cells and estimation of solar cell parameters using PSO algorithm, Renew. Energy 78 (2015) 105–113.

[14] H.M. Hasanien, Shuffled frog leaping algorithm for photovoltaic model identification, Sustain. Energy IEEE Trans. 6 (2015) 509–515.

[15] K. Ishaque, Z. Salam, An improved modeling method to determine the model parameters of photovoltaic (PV) modules using differential evolution (de), Sol. Energy 85 (2011) 2349–2359.

[16] K. Ishaque, Z. Salam, S. Mekhilef, A. Shamsudin, Parameter extraction of solar photovoltaic modules using penalty-based differential evolution, Appl. Energy 99 (2012) 297–308.

[17] L.L. Jiang, D.L. Maskell, J.C. Patra, Parameter estimation of solar cells and modules using an improved adaptive differential evolution algorithm, Appl. Energy 112 (2013) 185–193.

[18] W. Gong, Z. Cai, Parameter extraction of solar cell models using repaired adaptive differential evolution, Sol. Energy 94 (2013) 209–220.

[19] A.A. Elbaset, H. Ali, M. Abd-El Sattar, Novel seven-parameter model for photovoltaic modules, Sol. Energy Mater. Sol. Cells 130 (2014) 442–455.

[20] L.H.I. Lim, Y. Zhen, Y. Jiaying, Y. Dazhi, D. Hui, A linear identification of diode models from single I-V characteristics of PV panels, Ind. Electron. IEEE Trans. 62 (2015) 4181–4193.

[21] Ş.İ. Birbil, S.-C. Fang, An electromagnetism-like mechanism for global optimization, J. Glob. Optim. 25 (2003) 263–282.

[22] K. Price, R.M. Storn, J.A. Lampinen, Differential Evolution: a Practical Approach to Global Optimization, Springer Science & Business Media, 2006.

[23] P. Kaelo, M. Ali, Differential evolution algorithms using hybrid mutation, Comput. Optim. Appl. 37 (2007) 231–246.

[24] D.H. Muhsen, A.B. Ghazali, T. Khatib, I.A. Abed, Parameters extraction of double diode photovoltaic module's model based on hybrid evolutionary algorithm, Energy Convers. Manag. 105 (2015) 552–561.

[25] J. Liu, J. Lampinen, A fuzzy adaptive differential evolution algorithm, Soft Comput. 9 (2005) 448–462.

[26] R. Mallipeddi, P.N. Suganthan, Q.K. Pan, M.F. Tasgetiren, Differential evolution algorithm with ensemble of parameters and mutation strategies, Appl. Soft Comput. 11 (2011) 1679–1696.

[27] J. Brest, S. Greiner, B. Boskovic, M. Mernik, V. Zumer, Self-adapting control parameters in differential evolution: a comparative study on numerical benchmark problems, Evol. Comput. IEEE Trans. 10 (2006) 646–657.

[28] A.K. Qin, P.N. Suganthan, Self-adaptive differential evolution algorithm for numerical optimization, in: Evolutionary Computation, 2005. The 2005 IEEE Congress on, 2005, pp. 1785–1791.